Gas Sensors

Organic–Inorganic Hybrid Sol–Gel Materials Incorporating Functionalized Cobalt(III) Corroles for the Selective Detection of CO**

Jean-Michel Barbe, Gabriel Canard, Stéphane Brandès, and Roger Guilard**

Corroles and their metal derivatives continue to attract increasing interest because of their potential applications in many fields[1–3] and because of the development of new straightforward and powerful syntheses.[4–9] For example, it is now possible to functionalize the corrole macrocycle at the *meso* positions with several groups,[9,10] thus allowing it be anchored on various solid supports. Nanostructured organic–inorganic hybrid materials have also been developed, and these offer the possibility to incorporate many different organic chelates and complexes into their framework.[11–14] Moreover, immobilized complexes within the material are expected to be more stable than analogous isolated com-

[*] Dr. J.-M. Barbe, Dr. G. Canard, Dr. S. Brandès, Prof. Dr. R. Guilard
LIMSAG, UMR 5633
Faculté des Sciences "Gabriel"
Université de Bourgogne
6 Boulevard Gabriel, 21100 Dijon (France)
Fax: (+33) 380-396-117
E-mail: jmbarbe@u-bourgogne.fr
roger.guilard@u-bourgogne.fr

[**] This work was supported by the CNRS and Air Liquide. G.C. gratefully acknowledges the "Région Bourgogne" and Air Liquide for financial support.

Supporting information for this article is available on the WWW under http://www.angewandte.org or from the author.

 DOI: 10.1002/ange.200463009

plexes. Therefore, applications in different fields such as catalysis,[15] optical sensors,[16,17] and metal-ion separation processes, especially for transition metals,[18] heavy metals,[19,20] and actinides,[21] have been developed. Many examples of gas separation devices with hybrid organic–inorganic membranes based on a gas-diffusion process have been described,[22–24] but only a few examples of gas separation through the formation of chemical bonds between gas molecules and solid supports are known;[14,25] gas-detection studies with hybrid organic–inorganic materials are also rare.[17,26]

We recently reported the high affinity and infinite selectivity of cobalt(III) corroles for CO over O_2 and N_2.[27] Hybrid xerogels are able to combine the textural and the structural properties of the inorganic matrix such that the gas-binding properties of immobilized Co^{III} corroles can be tuned. Furthermore, the incorporation of these Co complexes in a solid inorganic network stabilizes the active species and the resulting materials are well adapted to the preparation of powders, fibers, or thin films. Unusual adsorption properties may arise by combining the intrinsic reactivity of the metallo–organic complex with the properties of the inorganic framework[28] as the arrangement of the organic moieties gives rise to short-range organization.[29,30] In this regard, corrole macrocycles were immobilized, for the first time, in a silica matrix through one Si–C covalent bond. The anchoring of one hydrolysable $-Si(OEt)_3$ terminal group to the corrole allowed the preparation of hybrid materials through a sol–gel process. Herein, we describe the synthesis, physicochemical characterization, and adsorption properties of these materials.

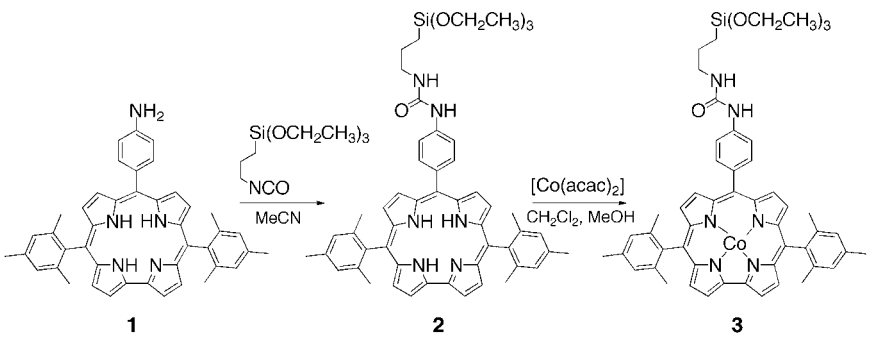

Scheme 1. Synthesis of the alkoxysilylated corrole precursors.

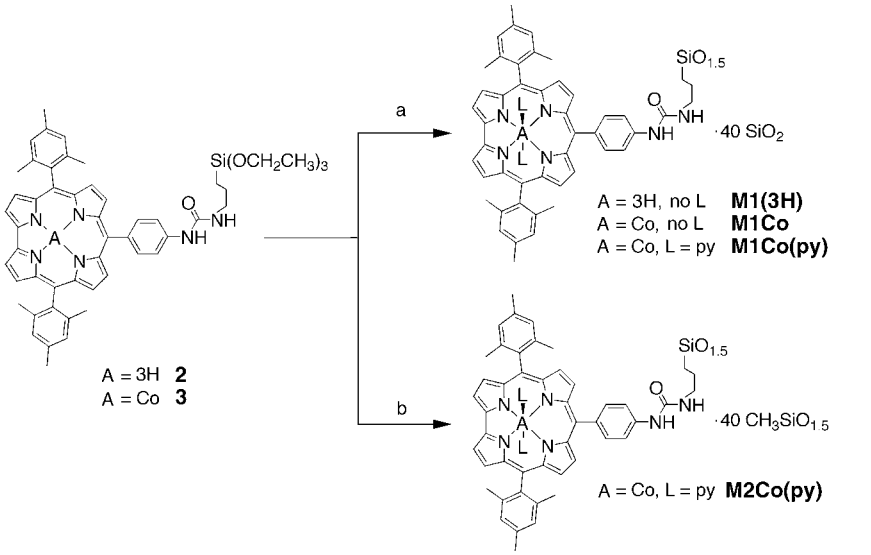

Scheme 2. Preparation of the materials: a) 40 equiv TEOS, distilled H_2O, TBAF, THF (with or without pyridine); b) 40 equiv MTEOS, distilled H_2O, TBAF, py, THF. L = axial pyridine ligand.

Complex **3** was prepared in two steps starting from corrole **1** (Scheme 1).[31] The reaction of 3-(triethoxysilyl)propyl isocyanate on **1** led to the formation of **2** in 4 days with a yield of 68%. Metalation of the free base **2** with cobalt(II) acetylacetonate afforded the precursor **3** in 96% yield (Scheme 1). These derivatives were characterized by ^{1}H NMR and UV/Vis spectroscopies, MALDI-TOF MS, and elemental analysis (see the Supporting Information).

Two types of materials were made: **M1** was prepared by co-polycondensation of **2** or **3** with 40 equivalents of tetraethoxysilane (TEOS); **M2** was prepared by co-polycondensation of **3** with 40 equivalents of methyltriethoxysilane (MTEOS; Scheme 2).[31] In the case of **M1**, the gelation process was performed at room temperature in THF by adding a stoichiometric amount of distilled water to the reaction mixture in the presence of tetrabutylammonium fluoride (TBAF, 1 mol% with respect to silicon) as catalyst. Under these conditions, **M1(3H)** and **M1Co**, which were obtained from **2** and **3**, respectively, gelled rapidly and the resulting monolithic gels were aged for 7 days. Upon addition of an excess of pyridine (py) during the gelation reaction of **3** with TEOS, **M1Co(py)** was synthesized (see Scheme 2 and the Supporting Information). The sol–gel process was further explored by treating the alkoxysilylated metallocorrole precursor **3** with 40 equivalents of MTEOS to prepare homogeneous molecular materials with enhanced stability of the cobalt(III) corrole in a moist atmosphere. A 14-day procedure led to the formation of **M2Co(py)** from a mixture of **3**, MTEOS, distilled water, a large excess of pyridine, and a catalytic amount of TBAF (5 mol% with respect to Si) at room temperature (Scheme 2). A larger TBAF/Si ratio was needed to initiate the sol–gel reaction for the formation of **M2Co(py)** than was needed for **M1Co(py)**.

The axial positions of the Co ion were protected during the sol–gel process by pyridine. The challenge was to make the Co^{III} coordination sites available for CO binding after removal of the pyridine ligands and to create a cavity for optimal accessibility of the gas. Thus, this protective method prevents inactivation of cobalt(III) corrole sites that occurs

through coordination of free silanol and siloxane groups on the material surface. The interaction of the cobalt ions with these groups cannot occur in **M2Co(py)** as there are mainly methyl groups present at the surface of the material.

The analytical and spectroscopic data for the silylated precursors and the hybrid xerogels are consistent with the structures presented in Scheme 2 and demonstrate that the corrole is incorporated into the solids. The metallocorrole concentration in the materials was deduced from elemental analyses (see the Supporting Information). For **M1Co**, the presence of the organic functional moieties in the mesopores and the condensation rate of the solids were evidenced by their ^{29}Si CP/MAS NMR spectra exhibiting one set of resonances at $\delta = -58$ and -63 ppm for the hybrid parts T^2 (C*Si*[(OSi)$_2$OH]) and T^3 (C*Si*[(OSi)$_3$]) substructures, respectively, and by the presence of a second set of resonances at $\delta = -101$ and -110 ppm corresponding to Q^3 (*Si*[(OSi)$_3$OH]) and Q^4 (*Si*[(OSi)$_4$]) inorganic substructures. Although the ^{29}Si CPMAS/NMR spectra could not be analyzed quantitatively, evidence of the major T^3 and Q^3 substructures was in accordance with a high condensation level for the solids.[32] Conversely, for **M2Co(py)**, only one sharp signal for the T^3 substructure was observed at $\delta = -66$ ppm, which is indicative of a polycondensed solid. The absence of signals between $\delta = -90$ ppm and -110 ppm suggests that no Si–C bond cleavage occured during the hydrolysis–polycondensation process.

The electronic spectra in the diffuse reflectance mode for **M1Co(py)** and **M1Co** materials resemble those of Co^{III} corroles in solution, with a single Soret band near 400 nm and very broad Q bands (500–650 nm; see the Supporting Information). These results indicate that the coordinating pyridine molecules are removed when the materials are put under vacuum. Conversely, the spectrum of **M2Co(py)** exhibits a new band close to 620 nm, which is characteristic of a hexacoordinated cobalt(III) corrole with two pyridine ligands.[33] Therefore, severe conditions are needed to remove pyridine molecules from **M2Co(py)**.

The surface area and pore diameters of the xerogels were determined by using nitrogen adsorption experiments according to BET and BJH calculations.[34,35] In general, the specific area is an important physical criteria for controlling accessibility of the gas molecules to the active sites. The texture of the free-base and cobalt(III) corrole materials obtained by co-gelation with TEOS was neither highly dependent on the presence of the metal in the macrocycle nor on the use of the protecting base. Thus, the surface areas of **M1(3H)**, **M1Co**, and **M1Co(py)** range between 450 and 520 m^{2}g^{-1}. The N_2 adsorption/desorption isotherms of these samples were of type II with no hysteresis loop, which is characteristic of macroporous materials.[36] In contrast, the **M2Co(py)** xerogel prepared with MTEOS was almost nonporous (12 m^{2}g^{-1}), even when more drastic aging conditions were used.

The CO adsorption was investigated concomitantly with O_2 and N_2 adsorption measurements to determine the selectivity of the materials towards CO versus O_2 and N_2. The equilibrium constant related to the CO binding affinity K_i and the adsorption capacity V_i (i = N_2 or O_2) was calculated by considering two different adsorption processes: selective chemisorption on the Co^{III} ion and nonselective physisorption resulting from dissolution and diffusion of the gas into the solid material.[27] The experimental isotherms corresponding to the CO adsorption were thus analyzed by using a model based on three Langmuir-type isotherms [Eq. (1)] and the N_2 and O_2 isotherms with a single Langmuir-type isotherm model [Eq. (2)].

$$V_{CO} = \frac{V_1 K_1 P}{1 + K_1 P} + \frac{V_2 K_2 P}{1 + K_2 P} + K_3 P \quad (1)$$

$$V_{i_{tot}} = \frac{V_i K_i P}{1 + K_i P} \quad (2)$$

An example of the CO adsorption adjustment by the isotherm model for **M1Co(py)** is given in Figure 1 along with experimental isotherms related to O_2 and N_2 adsorption. The main data relating to the CO adsorption for the four materials are reported in Table 1.

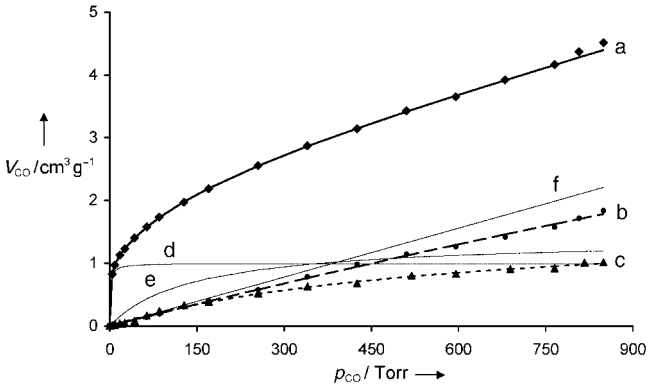

Figure 1. a) CO, b) N_2, and c) O_2 adsorption isotherms for **M1Co(py)** recorded at 293 K; d), e), and f) represent the first, second, and third components, respectively, of the calculated isotherms for CO adsorption (see [Eq. (1)].

Table 1: Experimental and calculated CO adsorption data for the xerogels

Material	V_{CO}[a] [cm^{3}g^{-1}]	V_1 [cm^{3}g^{-1}]	$(P_{1/2})_1$[b] [Torr]	V_2 [cm^{3}g^{-1}]	$(P_{1/2})_2$[b] [Torr]	$K_3 \times 10^3$ [Torr^{-1}]	[Co][c] [mmol g^{-1}]	% CO[d]
M1(3H)	0.84	2.42	895	–	–	–	–	–
M1Co	5.92	0.54	1.12	0.75	138	6.19	0.186	31
M1Co(py)	4.16	1.00	1.22	1.39	141	2.60	0.202	53
M2Co(py)	3.06	1.30	0.40	0.58	73	1.61	0.219	38

[a] Experimental volume adsorbed at 760 Torr. [b] $(P_{1/2})_i = 1/K_i$. [c] Concentration of cobalt in the materials. [d] Percentage of active sites calculated from $V_1 + V_2$ and [Co].

For CO adsorption, the first two Langmuir components are related to the chemisorption of CO on accessible cobalt(III) corroles located at the surface of the material (K_1) and on less accessible complexes inside the solid (K_2), K_1 being by far larger than K_2. Physisorption of CO on the solid is given by a third component (K_3). Figure 1 clearly shows that the N_2 (b) and O_2 (c) adsorptions correspond to physisorption of the

gases on the porous material ($P_{1/2}^{N_2 \text{ or } O_2} > 500$ Torr) as well as the third component of the CO experimental adsorption isotherm curve. Another key feature is the selectivity of the CO adsorption compared to those of O_2 and N_2. Indeed, these values, which are calculated from $(P_{1/2})_1^{O_2 \text{ or } N_2}/(P_{1/2})_1^{CO}$, are about 470 and 5600 for CO/O_2 and CO/N_2 respectively. These significant values represent the adsorption phenomenon at a very low partial pressure of CO and therefore at a very low CO content. However, from a chemical point of view, the CO/O_2 and CO/N_2 selectivities are infinite as O_2 and N_2 cannot bind to the Co^{III} ion.[27] Such an attribute is significant for a CO gas detector to be used under ambient conditions.

The adsorption of CO by **M1(3H)** (Table 1 and the Supporting Information) is very low and results only from physisorption on the solid. This is not surprising as **M1(3H)** incorporates a free-base corrole, therefore no chemisorption of CO can occur. Furthermore, it is clear that the introduction of pyridine during the gelation process significantly increases the accessibility of the Co^{III} sites as demonstrated by the higher V_1 and lower $(P_{1/2})_1$ values for **M1Co(py)** and **M2Co(py)** compared with **M1Co** (see Table 1). Moreover, the use of MTEOS instead of TEOS induces an important decrease in the physisorption of CO, which is reflected by a lower K_3 value (Table 1) while maintaining a high accessibility of the metallocorroles, as shown by the low V_2 value with respect to V_1. Thus, a large surface area is not a prerequisite for a material that is very reactive towards CO.

In conclusion, very high affinities for CO compared with O_2 and N_2 were obtained for Co^{III} corroles incorporated into silica matrices. The sol–gel process led to new organic–inorganic hybrid composite materials. By this flexible process, devices with different shapes might be prepared, such as thin films coated on a solid support through a gelation reaction. This development facilitates the elaboration of a gas sensor and enhances the long-term stability of the device.

Received: December 21, 2004
Published online: April 14, 2005

Keywords: carbon monoxide sensors · cobalt · organic–inorganic hybrid composites · porphyrinoids · sol–gel processes

[1] R. Paolesse in *The Porphyrin Handbook*, *Vol. 2* (Eds.: K. M. Kadish, K. M. Smith, R. Guilard), Academic Press, New York, **2000**, p. 201.
[2] C. Erben, S. Will, K. M. Kadish in *The Porphyrin Handbook*, *Vol. 2* (Eds.: K. M. Kadish, K. M. Smith, R. Guilard), Academic Press, New York, **2000**, p. 233.
[3] R. Guilard, J. M. Barbe, C. Stern, K. M. Kadish in *The Porphyrin Handbook*, *Vol. 18* (Eds.: K. M. Kadish, K. M. Smith, R. Guilard), Elsevier, New York, USA, **2003**, p. 303.
[4] Z. Gross, N. Galili, I. Saltsman, *Angew. Chem.* **1999**, *111*, 1530; *Angew. Chem. Int. Ed.* **1999**, *38*, 1427.
[5] D. T. Gryko, *Chem. Commun.* **2000**, 2243.
[6] R. Paolesse, S. Nardis, F. Sagone, R. G. Khoury, *J. Org. Chem.* **2001**, *66*, 550.
[7] D. T. Gryko, K. Jadach, *J. Org. Chem.* **2001**, *66*, 4267.
[8] D. T. Gryko, K. E. Piechota, *J. Porphyrins Phthalocyanines* **2002**, *6*, 81.
[9] D. T. Gryko, B. Koszarna, *Org. Biomol. Chem.* **2003**, *1*, 350.
[10] R. Guilard, D. T. Gryko, G. Canard, J. M. Barbe, B. Koszarna, S. Brandès, M. Tasior, *Org. Lett.* **2002**, *4*, 4491.
[11] G. Dubois, C. Reyé, R. J. P. Corriu, S. Brandès, F. Denat, R. Guilard, *Angew. Chem.* 2001, 113, 1121; *Angew. Chem. Int. Ed.* **2001**, *40*, 1087.
[12] R. J. P. Corriu, F. Embert, Y. Guari, C. Reyé, R. Guilard, *Chem. Eur. J.* **2002**, *8*, 5732.
[13] M. G. Basallote, E. Blanco, M. Blazquez, M. J. Fernandez Trujillo, R. Litran, M. A. Manez, M. R. del Solar, *Chem. Mater.* **2003**, *15*, 2025.
[14] R. J. P. Corriu, E. Lancelle-Beltran, A. Mehdi, C. Reyé, S. Brandès, R. Guilard, *Chem. Mater.* **2003**, *15*, 3152.
[15] A. Adima, J. J. E. Moreau, M. Wong Chi Man, *Chirality* **2000**, *12*, 411.
[16] S. Blair, R. Kataky, D. Parker, *New J. Chem.* **2002**, *26*, 530.
[17] C. Sanchez, B. Lebeau, F. Chaput, J.-P. Boilot, *Adv. Mater.* **2003**, *15*, 1969.
[18] H. J. Im, Y. Yang, L. R. Alain, C. E. Barnes, S. Dai, Z. Xue, *Environ. Sci. Technol.* **2000**, *34*, 2209.
[19] A. G. S. Prado, L. N. H. Arakaki, C. Airoldi, *J. Chem. Soc. Dalton Trans.* **2001**, 2206.
[20] A. Walcarius, C. Delacote, S. Sayen, *Electrochim. Acta* **2004**, *49*, 3775.
[21] S. Bourg, J.-C. Broudic, O. Conocar, J. J. E. Moreau, D. Meyer, M. W. C. Man, *Chem. Mater.* **2001**, *13*, 491.
[22] C. Guizard, A. Bac, M. Barboiu, N. Hovnanian, *Sep. Purif. Technol.* **2001**, *25*, 167.
[23] D.-W. Lee, B. Sea, K.-Y. Lee, K.-H. Lee, *Ind. Eng. Chem. Res.* **2002**, *41*, 3594.
[24] K. Kuraoka, Y. Tanaka, M. Yamashita, T. Yazawa, *Chem. Commun.* **2004**, 1198.
[25] G. Dubois, R. Tripier, S. Brandès, F. Denat, R. Guilard, *J. Mater. Chem.* **2002**, *12*, 2255.
[26] E. S. Ribeiro, Y. Gushikem, J. C. Biazzotto, O. S. Serra, *J. Porphyrins Phthalocyanines* **2002**, *6*, 527.
[27] J.-M. Barbe, G. Canard, S. Brandès, F. Jérôme, G. Dubois, R. Guilard, *Dalton Trans.* **2004**, 1208.
[28] R. Corriu, C. Reye, A. Mehdi, G. Dubois, C. Chuit, F. Denat, B. Roux-Fouillet, R. Guilard, G. Lagrange, S. Brandès, WO Pat. 9937656, **1999**; J. Goulon, C. Goulon-Ginet, A. Rogalev, F. Wilhelm, N. Jaouen, D. Cabaret, Y. Joly, G. Dubois, R. J. P. Corriu, G. David, S. Brandès, R. Guilard, *Eur. J. Inorg. Chem.*, in press.
[29] B. Boury, R. J. P. Corriu, *Chem. Commun.* **2002**, 795.
[30] B. Boury, R. J. P. Corriu, *Chem. Rec.* **2003**, *3*, 120.
[31] Abbreviations: compound **1**: 5,15-dimesityl-10-(4-aminophenyl)corrole; compound **2**: 5,15-dimesityl-10-{4-phenyl-[3-(3-triethoxysilyl)propyl]urea}corrole; compound **3**: [5,15-dimesityl-10-{4-phenyl-[3-(3-triethoxysilyl)propyl]urea}corrolato] cobalt(III); acac: acetylacetonate; TEOS: tetraethoxysilane; MTEOS: methyltriethoxysilane; TBAF: tetrabutylammonium fluoride.
[32] D. A. Loy, K. J. Shea, *Chem. Rev.* **1995**, *95*, 1431.
[33] R. Guilard, C. P. Gros, F. Bolze, F. Jérôme, Z. Ou, J. Shao, J. Fischer, R. Weiss, K. M. Kadish, *Inorg. Chem.* **2001**, *40*, 4845.
[34] S. Brunauer, P. H. Emmet, E. Teller, *J. Am. Chem. Soc.* **1938**, *60*, 309.
[35] E. Barrett, L. G. Joyner, P. P. Halenda, *J. Am. Chem. Soc.* **1951**, *73*, 373.
[36] K. S. W. Sing, D. H. Everett, R. A. W. Haul, L. Moscou, R. A. Pierotti, J. Rouquérol, T. Siemieniewska, *Pure Appl. Chem.* **1985**, *57*, 603.

